JOURNAL OF APPLIED BIOANALYSIS, May 2025, p. 344-352.
http://doi.org/10.53555/jab.v11i2.214 (ISSN 2405-710X)
Vol. 11, No. 2

OPEN ACCESS

Lagerstroemia Speciosa (Banaba) Plant Extract Mediated Green Synthesis Of Ni Doped Ag Nanoparticles Characterisations And Their Biological Activities

G. Bhagyalaxmi[1], K. Suresh babu[2], Ranjith Kumar Nadipalli[2], K. Ramamurthy[1*], R.A. Kalaivani[1]

[1]*Department of chemistry, Vels Institute of Science, Technology & Advanced Studies (VISTAS), Pallavaram, Chennai, India.*
[2]*Department of chemistry, Marri Laxman Reddy Institute of Technology and Management, Dundigal, Hyderabad*

***Corresponding Author:** K. Ramamurthy*
**Email: kramchem1988@gmail.com*

Abstract

Chemistry The purpose of this research was to use extract from the Banaba plant to create nickel-silver (Ni-Ag) nanoparticles (NPs) that are safe for the environment. Spectroscopic methods such as UV-Visible spectroscopy, Powder X-ray diffraction (XRD), Fourier transform infrared (FTIR) analysis, scanning electron microscopy (SEM), and Raman spectroscopy will be used to characterise these synthesised nanoparticles. The absorbance peak associated with silver nanoparticles was 427 nm. The XRD analysis reveals the presence of different phases. The photocatalytic properties of Ni-Ag nanoparticles are therefore a result of their green production. Clearly, this aids in the investigation of Ni-Ag nanoparticles for a variety of potential applications. FTIR to determine their size, stability, number of functional groups, particle structure, and existence of Ni-Ag particles, respectively. The scanning electron microscopy (SEM) analysis of Ni-Ag nanoparticles revealed their uniformly spherical shape and Raman Spectroscopy uncovers intricate details on molecular interactions, polymorphology, and crystallinity using a non-destructive chemical analysis method. The antibacterial effects of the Banaba plant-mediated Ni-Ag NPs are very efficient against two different types of bacteria. These results seem to be crucial from a therapeutic, pharmacological, and environmental perspective.

Keywords: Lagerstroemia Speciosa (Banaba) plant, Plant extract, silver nanoparticles, nickel nitrate, anti-microbial.

Introduction

The unique possible uses of metal nanoparticles in electronics, optoelectronics, data storage, medication administration, and magnetics have made their synthesis a hot subject in contemporary material science research in recent years (Sundararajan & Kumari, 2014). In the treatment of common medical conditions, such as diabetes, cancer, and fever, medicinal plants play a key part in the lives of 800 million people worldwide (Motitswe, 2021). As a result of the wide variety of nanoscale physical characteristics shown by nanomaterials, green synthesis' incorporation into nanotechnology has garnered considerable interest (Karthik et al., 2024). Emerging from the realm of multidisciplinary study is the discipline of nanoscience and technology (Shereen et al., 2024).

Treatments for cancer and diabetes make use of nanoparticles as carriers because they greatly enhance the efficacy oftarget-specific medication delivery. An environmentally benign approach to synthesising metal nanoparticles, "green synthesis" uses less hazardous by-products. At the same time, they enhance the synthetic particles' therapeutic properties. There may be biomedical uses for the Ni-Ag NPs. When compared to physical and chemical approaches, biological synthesis of Ni-Ag NPs offers several benefits, including large-scale commercial production, compatibility with medical and pharmaceutical applications, and cost-effectiveness (Chandrakala et al., 2021).

Treatments for cancer and diabetes make use of nanoparticles as carriers because they greatly enhance the efficacy oftarget-specific medication delivery. An environmentally benign approach to synthesising metal nanoparticles, "green synthesis" uses less hazardous by-products. At the same time, they

enhance the synthetic particles' therapeutic properties. There may be biomedical uses for the Ni-Ag NPs. When compared to physical and chemical approaches, biological synthesis of Ni-Ag NPs offers several benefits, including large-scale commercial production, compatibility with medical and pharmaceutical applications, and cost-effectiveness (Chandrakala et al., 2021). There is a vast variety of secondary metabolites found in medicinal plants that have medicinal uses. In this work, we used Banaba plant extracts to decrease Ni-Ag salts and produce Ni-Ag nanoparticles (Prakash et al., 2021).

Banaba and Jarul are popular names for the same species of Lagerstroemia, which is in the Lythraceae family. It has a long history of praise as a therapeutic herb (Gupta et al., 2018). Treatments for diabetes mellitus, renal illness, stomach discomfort, fever, urinary infection, decongestion, diarrhoea, mouth ulcers, and other conditions have been largely shown to be effective using this plant. Banaba, a member of the Lythraceae family, is a medicinal attractive plant with vividly coloured blossoms of pink or purple. Cultivated extensively, it is plentiful in tropical and subtropical areas of South and Southeast Asia, as well as in Japan, the Philippines, Indonesia, Vietnam, Cambodia, Myanmar, Thailand, and the rest of Vietnam. Detailed description A medium-sized evergreen tree, the banaba may reach a height of 30 metres. The surfaces of the opposing, leathery leaves the subglobose fruit is around 2.5 cm long and has a firm, woody exterior (Al-Snafi, 2019).

There are wings on the seeds. The Swedish scientist Magnus von Banaba, who brought Linnaeus specimens from the East, was the one who first noticed the name Banaba. One of its frequent names among Indians is "Pride of India," but it goes by the names Giant crape myrtle as well (Zahoor et al., 2023).The current study details the environmentally friendly productionof Ni- Ag nanoparticles (Ls-Ni-Ag NPs) using an ethanolic extract of L. speciosa and their evaluation for antibacterial properties (Koduru et al., 2021).
This plant is classified as semi-deciduous. Various active metabolites, including steroids, terpenoids, glycosides, phenolic compounds, α- amino acids, saponins, starch, alkaloids, carbohydrates, organic acids, flavonoids, reducing sugars, tannins, and many more, were discovered during the phytochemical examination of the Banaba plant (Qaeed, 2023).

Banaba has a wide variety of pharmacological effects, including those on the immune system, cardiovascular system, gastrointestinal tract, thrombolytic effects, antioxidant properties, anticancer effects, hypolipidemic effects, anti-obesity, inflammation, pain, and many more. Few results on the green synthesis of Ni-Ag NPs Lagerstroemia speciosa utilising extract and their biological activities have been published, despite the abundance of research papers on the synthesis and characterisation of Ni-AgNPs in the literature. The objective of this study was to investigate the antibacterial and microbiological activity of Ni-AgNPs synthesised from Banaba plant extract using a biogenic method (Tandrasasmita, 2023).

Materials and methods

Plant sample collection: The *Speciosa* stem were collected from the Tirumala Forest from madhavachetti herbium keeper India was taken that the sample were healthy and had no insect growth on it. The plant material (Figure 1) was cleaned thoroughly 2-3 times with distilled water, dried in a shady place and then grinded into fine particles with a help of mortar and pestile. It is a plant powder compound. sieved and stored in airtight container (Devi et al., 2019).

Figure 1

The quantitative amount of powder (Figure1) was used for extraction by using Soxhlet extractor. Solvents of increasing polarity (hexane, chloroform and methanol, ethanol) were used to carry out successive solvent extraction.

Chemicals used: The following items were acquired from UV Scientific Enterprises: silver nitrate, nickel nitrate deionized water. No further processing was performed on any of the compounds; they were all of analytical grade and of the greatest purity.

Preparation of the L. Speciosa plant (banaba) extract:

A mixture of five grammes of dried ground plant material, one hundred millilitres of deionized water, and fifty millilitres of ethanol solvent was stirred continuously for eight hours at room temperature using a magnetic stirrer set at 500 revolutions per minute. After that taken out from the stirrer filtered that compound Using Whatman No. 1 filter paper filtration was done to produce the aqueous plant extraction (Rahman et al., 2020). It is used to synthesis of nano particles.

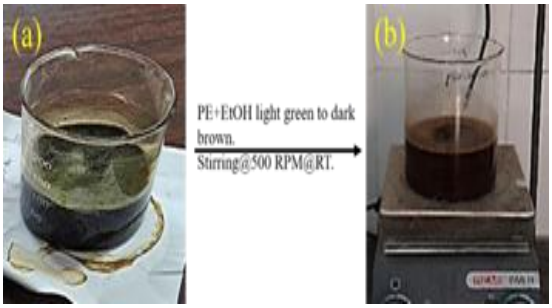

Figure 2

Synthesis of Ni-Ag NPs with using L. Speciosa (Banaba):

To make the green method of nanoparticles, dissolve 1 gramme of silver nitrate in 25 millilitres of water and 1 milligramme of nickel oxide in 25 millilitres of water. Combine the two solutions in a 1000 millilitre beaker and stir with a magnetic stirrer for 10 minutes. Next, fill the burette with 50 millilitres of plant solution. Once again, stirring continually for half an hour, and then releasing the plant solution drop by drop until it is eaten (Figure 2). Figure.2 shows that the solution's colour changed from light yellow to dark brown when the nanoparticles were removed from the stirrer (Shashiraj et al., 2023). The reaction mixture needed to be heated more until the solvent evaporated, therefore the mantle was heated further. The solid powder component was obtained by letting the solution cool to room temperature and then collecting the supernatant. To isolate the NPs in their as-synthesized state (pre-heated plant extract), the supernatant was then spun at 12,000 rpm for 10 minutes. Deionized water was used to wash the NPs thrice in a row. After you get the XRD, UV, FTIR, Raman, and SEM results for the Ag-Ni nano plant powder, weigh it and send it on to the characterization phase (Wang et al., 2023). Turn the compound into a powder by heating it to 300 ºC and above. submit for characterization (heated plant extract) (Jain, 2019).

To make the green method of nanoparticles, dissolve 1 gramme of silver nitrate in 25 millilitres of water and 1 milligramme of nickel oxide in 25 millilitres of water. Combine the two solutions in a 1000 millilitre beaker and stir with a magnetic stirrer for 10 minutes (Banerjee et al., 2014). Next, fill the burette with 50 millilitres of plant solution. gradually releasing the plant solution till it is completely digested. The solution's hue changes as time passes when silver salt is mixed with plant extracts. Once again, fill the burette with 17 mL of NaOH solution (the reducing agent). Slowly pour the solution up to the base into the beaker, which is set on a magnetic stirrer. Stir constantly for another 1.5 hours. After then, it is removed from the stirrer. The reaction mixture needed to be heated more until the solvent evaporated, therefore the mantle was heated further. The hue shift from colourless to brown signified the complete reduction of AgNO3 to Ag+ ions. The mixture was let to cool until it reached room temperature. get a powder compound that is solid. and then the liquid on top was gathered. To separate the NPs that were synthesised, the supernatant was centrifuged at 12,000 rpm for 10 minutes. Deionized water was used to wash the NPs thrice in a row. After obtaining the XRD UV, FTIR, Raman, SEM, and Ni-Ag nano plant powder, weigh the samples and submit them to the characterization lab for analysis (plant extract with NaOH). Powder the component by heating it to 300 ºC (Plant extract with NaOH after heating). For characterisation, send (Widdatallah et al., 2020).

Characterisation of the Ni-Ag NPs:

Using a 1 cm glass cuvette, the hydrosol samples were subjected to ultraviolet-visible spectroscopy on a spectrophotometer. To detect the adsorption, we used a UV-Vis spectrophotometer (Shimadzu, Japan) with quartz cells. To stir the solutions, we used a magnetic stirrer and a heater. To conduct the photocatalyst test, we used a UV-A lamp 11
W. To adjust the pH, we used a pH metre. Analysis using a scanning electron microscope (SEM) was carried out. To prepare the samples, the copper grid was dipped into the NP hydrosol and let to evaporate. Next, an X-ray diffractometer was used to examine the powdered and dried samples by means of XRD. A spectrophotometer was used to conduct the FTIR studies.

Results and discussion

Concurrent reduction of Ag+ and NiO in the presence of Banaba plant extract was used to synthesise the Ni-Ag alloy NPs. In this synthesis by addition of reductive agent sodium hydroxide acts as reductive agent.

XRD Analysis

XRD analysis was utilized to investigate the structural properties and crystalline composition of Nickel doped silver nanoparticles. The XRD pattern of Ni doped Ag NPs, derived from plant extract, is illustrated in Figure A (combined XRD graph). The observed peaks at 32.47°, 37.93°, 44.60°, 64.77°, 77.32°,81.48°, 32.83°, 46.75°, 58.0° correspond to the crystallographic planes 122, 111, 200, 220, 311, 222, 122, 231, 241 respectively (Kanthesh, 2018).

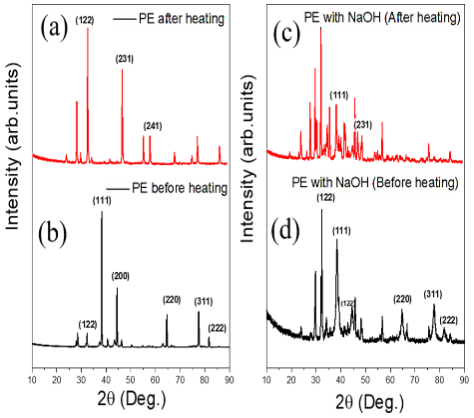

Figure 3

(Figure 3(b))These diffraction peaks align with the JCPDS No. 04-0783 standard database values. The crystallite size of Ni doped Ag NPs, computed via the Scherrer equation using the highest diffraction peak attributed to the (111) crystal planes, is approximately 38.4 positions. The X-ray diffraction analysis reveals peaks spanning from 36.74 to 39.13°, with the highest intensity observed at 38.45° (Figure3(a)– Crystallite size cal). The particle size distribution for two samples is 55.15 nm and 47.42 nm. XRD analysis was utilized to investigate the structural properties and crystalline composition of Nickel doped silver nanoparticles. The XRD pattern of Ni doped Ag NPs, derived from plant extract (combined XRD graph). The observed peaks at 32.27°, 38.68°, 44.36°, 64.84°, 77.37°,81.71°, 37.98°, 46.72° correspond to the crystallographic planes 122, 111, 122, 311, 222, 111,231(Figure 3(c)) respectively. These diffraction peaks align with the JCPDS No. 04-0783 standard database values. The crystallite size of Ni doped Ag NPs (Jain, 2017), computed via the Scherrer equation using the highest diffraction peak attributed to the (111) crystal planes, is approximately 38.4 positions. The X-ray diffraction analysis reveals peaks spanning from 36.74 to 39.13°, with the highest intensity observed at 38.45° (Figure 3(d)Table – Crystallite size cal.). The particle size distribution for two samples is 217.82 nm and 47.87 nm.

UV-Vis analysis

The UV-vis absorption behaviour of Ni doped silver NP samples was analysed to determine the optical band gap.

The samples showed increased absorption towards shorter wavelengths, particularly in the UV region (Figure 4(a), after heat treatment. The absorption edge wavelengths were found to be 311 nm, 314 nm, 402 nm and 412 nm, indicating a shift towards lower wavelengths possibly due to a decrease in particle size (Dhama & Tiwari, 2014). (Figure 4(b)) The Tauc equation (α h ν) 1 / n = A (h ν − Eg) discusses optical absorption parameters such as α, A, h, υ, n, and Eg. Band gap energy of Ni doped silver NPs was calculated by extrapolating a graph of "hυ" and (αhυ)2, showing an increase in band gap energy with heat-treatment, (Figure 4(d)) possibly due to differences in particle size. The band gap energy of Ni doped silver nanoparticles increases with heat treatment, reaching values of 2.7 eV and 2.5 eV. This is thought to be due to variations in particle size. The UV-vis absorption characteristics of Ni- doped silver NP samples were examined to assess the optical band gap. Analysis of the UV- vis spectra of both pre- and post-heat treatment samples revealed heightened absorption, particularly in the UV range and towards shorter wavelengths (Figure 4(c)). The absorption edge wavelengths for the samples were determined to be 307 nm, 312 nm, 375 n and 377 nm respectively. This shift towards lower wavelengths in absorption bands could be indicative of a reduction in particle size.

$$(\alpha\ h\ \nu)\ 1\ /\ n = A\ (h\ \nu - E\ g)$$

The Tauc equation discusses optical absorption parameters, and the band gap energy of Ni doped silver nanoparticles increases with heat treatment, possibly due to differences in particle size. Heat treatment of Ni doped silver nanoparticles results in an increase in band gap energy, reaching value of 1 eV. This is believed to be caused by changes in particle size.

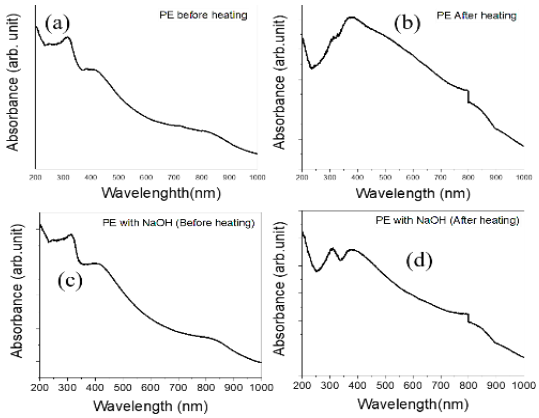

Figure 4

FTIR analysis:

We used Fourier transform infrared spectroscopy (FTIR) to look for reductive groups like CLC, (NH)CLO (proteins and amino acids), or -OH (phenols) in the Banaba plant extract; these groups could be reducing the metal precursors or bioreducing the nanoparticles (NPs). Important reductants that convert nickel oxide and Ag+ include polyphenols, reducing sugars, and flavonoids. For their part, proteins play a gentle protective role in the environmentally friendly production of metals (Sandhu, 2013). Polyphenols, flavonoids, reducing sugars, proteins, and other chemicals are the main components of the Banaba plant extract, according to intensive investigations. Molecular vibrations and

functional groups are identified by distinctive peaks and bands in Fourier transform infrared spectra. 1459 nm-1 One possible explanation for this peak is because aromatic compounds have stretching vibrations in their C=C bonds. This frequency, 1350 cm-1, may be indicative of aromatic compound or methyl group bending vibrations. This frequency, which might be 1042 cm-1, could be associated with the stretching vibration of C-O bonds in ethers, alcohols, or esters. figures 5(a) shows 877 cm-1 Possible metal-oxygen (Ni-O) or metal-silver (Ag) links, as well as metal-ligand stretching vibrations, could be indicated by this peak. 834 cm-1: This peak may represent out-of-plane bending vibrations or the bending vibration of C-H bonds in aromatic molecules.

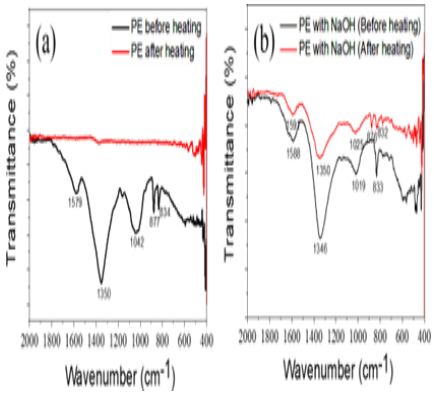

Figure 5

Interpretation of an FTIR spectrum (Prajwala & Raghu, 2019) involves identifying these characteristic peaks and correlating them with known functional groups or molecular structures to determine the composition of the sample.

1591 cm-1 This peak might correspond to the stretching vibration of C=C bonds in aromatic compounds. 1588 cm-1 Similarly to 1591 cm-1, (Figure 5(b)) this frequency could indicate the presence of C=C bonds in aromatic compounds. 1346 cm-1This peak might indicate the presence of bending vibrations of C-H bonds in aromatic compounds or methyl groups (Agarwal & Priyadarshini, 2019). 1350 cm-1Similarly to 1346 cm-1, this frequency could indicate the presence of bending vibrations of C-H bonds in aromatic compounds or methyl groups. 1025 cm-1: This frequency might correspond to the stretching vibration of C-O bonds in ethers, alcohols, or esters. 1019 cm-1: Similarly to 1025 cm-1, this peak could indicate the stretching vibration of C-O bonds in ethers, alcohols, or esters. 876 cm- 1 This peak might indicate the presence of metal-ligand stretching vibrations, possibly metal- oxygen (Ni-O) or metal-silver (Ag) bonds. 833 cm-1: This peak could indicate the bending vibration of C-H bonds in aromatic compounds or out-of-plane bending vibrations. 832 cm-1: Similarly to 833 cm-1, this frequency could indicate the bending vibration of C-H bonds in aromatic compounds or out-of-plane bending vibrations (Singh & Panghal, 2014).

Raman analysis

The Raman peaks in Ni-doped silver nano samples indicate the presence of different vibrational modes and bonds such as lattice vibrations, phonons, metal-ligand bonds, and carbon-carbon bonds. The interpretation of these peaks can vary based on the sample's chemical composition, crystal structure, and bonding environment within the material. 456 cm-1 This peak might correspond to lattice vibrations, phonons, or possibly vibrations involving metal-ligand bonds, such as silver-oxygen (Ag-O) or nickel-oxygen (Ni-O) bonds (Dev, 2018) 531 cm-1.

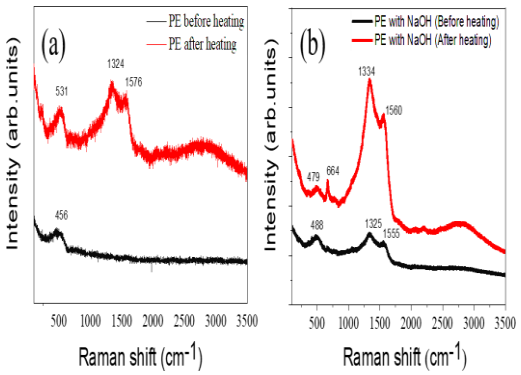

Figure 6

This frequency could correspond to lattice vibrations, phonons, or possibly vibrations involving metal-ligand bonds, such as silver-oxygen (Ag-O) or nickel-oxygen (Ni-O) bonds. 1324 cm-1: This peak might correspond to lattice vibrations or phonons in the crystal structure of the material. 1576 cm-1This frequency could correspond to vibrational modes involving aromatic carbon-carbon (C=C) bonds or possibly metal-ligand bonds. The Raman experimental spectrum displays a vibration of 1334 cm-1: This peak might correspond to lattice vibrations or phonons in the crystal structure of the material. 1560 cm-1: This frequency could correspond to vibrational modes involving aromatic carbon-carbon (C=C) bonds or possibly metal-ligand bonds. 1325 cm-1: This peak might correspond to lattice vibrations or phonons in the crystal structure of the material. 1555 cm-1: This frequency could correspond to vibrational modes involving aromatic carbon-carbon (C=C) bonds or possibly metal-ligand bonds. 479 cm-1: This peak might correspond to lattice vibrations, phonons, or possibly vibrations involving metal- ligand bonds, such as silver-oxygen (Ag-O) or nickel-oxygen (Ni-O) bonds. 488 cm-1 (Balouiri, 2016). Similarly to 479 cm-1, this frequency might also correspond to lattice vibrations, phonons, or vibrations involving metal-ligand bonds. 664 cm-1This peak might correspond

to lattice vibrations or phonons in the crystal structure of the material.

Dielectric

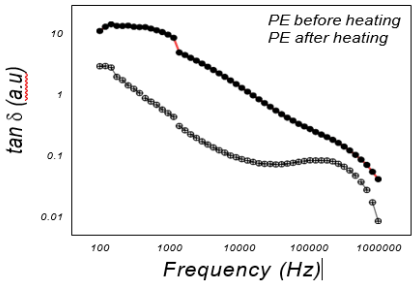

Figure 7

The plots show changes in dielectric constant and loss tangent as Ni dopant content increases, with curves flattening out and ε' decreasing. This parameter is crucial for characterizing dielectric properties.The drop in ε' with Ni addition is linked to reduced Ni-Ag NPs value. Impedance spectroscopy is used to study conductivity of nanocomposites, with Z' values decreasing as frequency increases32.Dielectric constant declines rapidly with increasing frequency due to diminishing space charge polarization, stabilizing at nearly constant values but increasing with temperature. At lower frequencies, dielectric constant remains.

The plots illustrate variations in dielectric constant and loss tangent with increasing Ni dopant content, showing flattened curves and a decrease in ε'. This parameter is pivotal for understanding dielectric properties. The decline in ε' with Ni addition is associated with a reduced value of Ni-Ag NPs. Impedance spectroscopy is employed to examine the conductivity of nanocomposites, revealing decreasing Z' values with increasing frequency. Dielectric constant decreases rapidly with frequency escalation due to diminishing space charge polarization, eventually stabilizing at nearly constant values but exhibiting an increase with temperature. At lower frequencies, the dielectric constant remains elevated. (Figure7(a)) Impedance spectroscopy is a useful method for analysing the conductivity of nanocomposites. The real part of impedance decreases with frequency, indicating insulating behaviour and polarization effects. Resistance and relative permittivity also decrease with frequency, with polarization effects becoming less synchronized at higher frequencies. Doping content influences relative permittivity, while orientation and interfacial polarization are important factors. Additionally, the loss tangent in nanocomposites increases with frequency due to polarization loss from dipole reorientation. (Figure7(b)).

SEM analysis

Using a field emission scanning electron microscope, the spherical form of the Ni-Ag nanoparticles was observed. Various magnifications (50X, 100X) were used to examine these nanoparticles.

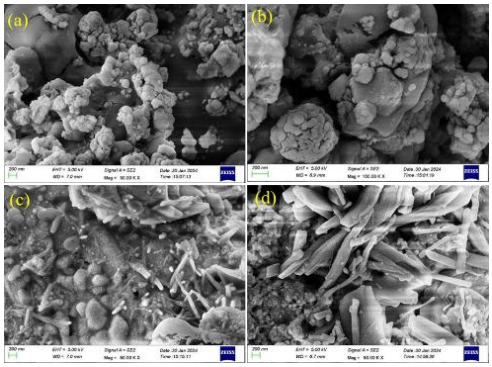

Figure 8

Comparison between antimicrobial activity of L. speciosa plant extract and Ni-Ag NPs using plant extract of L. speciosa.

Antimicrobial activity of L. speciosa

It was shown that Methanolic extracts of Lagerstroemia speciosa leaves (MLL) and barks (MBL) have antibacterial activity against eleven harmful bacteria and three fungi. The antibacterial activity of MLL was shown to be moderate to very good against gramme positive bacteria, with an average zone of inhibition of 13±0.93 -16 ±0.76 mm. On the other hand, it was found to be good to outstanding against gramme negative bacteria, with a zone of inhibition of 10 ±0.19 -20±1.65 mm. When tested against V. mimicus, the greatest zone of inhibition was 20±1.65 mm, whereas P. aeruginosa demonstrated a minimum zone of inhibition of 10±0.19 mm. Once again, MBL demonstrated acceptable to outstanding antibacterial action against gram-positive bacteria, with an average zone of inhibition of 14±1.55-18 ±0.20 mm, and good to excellent action against gram-negative bacteria, with a zone of inhibition ranging from 12±0.13 - 21±0.15 mm. The greatest zone of inhibition against V. mimicus was 21±0.15 mm, whereas the lowest zone of inhibition against P. aeruginosa was 120.13 mm.

In previous research on fungi, MBL had excellent antifungal activity (17±1.77 -19±0.32 mm, zone of inhibition), whereas MLL exhibited moderate antifungal activity (12±1.45 -14±1.06 mm, zone of inhibition).The rise of antibiotic-resistant bacteria and other microbes, as well as the negative consequences of synthetic antibiotics, have led many to turn to medicinal plants as a safer and more effective alternative for treating bacterial illnesses. Both MBL and MLL exhibited strong antibacterial activity against bacteria and fungus, according to the current study's antimicrobial activity results, which may indicate the existence of antimicrobial

substances. The presence of tannins, steroids/ triterpinoids, and flavonoids in L. speciosa leaves was discovered in previous phytochemical investigations (Woratouch et al., 2011). Infectious diseases could be effectively treated with this plant, and tannins have antioxidant and protein-precipitating properties. It has been shown that plants produce flavones in reaction to microbial infection.

These compounds disrupt the metabolism of microbes by creating an osmotic imbalance, denaturing enzymes, and altering ion channels (Havsteen, 2002). The antibacterial effect of MBL and MLL is attributed to their high total phenolic component content. It is believed that oxidised chemicals block enzymes, either by reactivity with sulfhydryl groups or through less specific interactions with proteins, and that this is the mechanism by which phenolic toxins harm microbes. The extracts were more effective against gram-negative bacteria than gram-positive bacteria, regardless of whether the bacteria were gramme positive or negative. One possible explanation is that the components of the cell walls of the two groups are structurally different. While both MBL and MLL showed promise as antifungal agents, MBL proved to be the more effective of the two.

Table 1

Name of the Test organisms	Diameter of zone of inhibition Mean (mm) ± SD		
	MBL (500µg/disc)	MLL (500µg/disc)	Kanamycin (30µg/disc)
Gram positive bacteria			
Bacillus subtilis	17 ±0.87	14 ±2.05	28 ±0.67
Bacillus megaterium	13 ±0.34	13 ±0.93	33 ±1.05
Sarcina lutea	13 ±0.05	16 ±0.55	30 ±0.03
Staphylococcus aureus	18 ±0.20	13 ±1.02	28 ±1.22
Bacillus cereus	14 ±1.55	16 ±0.76	32 ±0.44
Gram negative bacteria			
Salmonella paratyphi	19 ±1.97	14 ±0.32	30 ±0.76
Vibrio mimicus	21 ±0.15	20 ±1.65	35 ±.23
Vibrio parahemolyticus	14 ±0.39	12 ±2.23	33 ±0.3
Pseudomonas aeruginosa	12 ±0.13	10 ±0.19	28 ±2.13
Escherichia coli	18 ±0.44	16 ±00	30 ±1.88
Shigella dysenteriae	18 ±1.72	17 ±2.32	30 ±00

The values are expressed as Mean ±standard deviations (SD). "-" Indicates no zone of inhibition

In vitro antibacterial activity of the methanol extracts of L. speciosa (leaves & barks) and kanamycin discs.

Table 2

Test Organisms	MBL	MLL
Aspergillus niger	19 ±0.00	12 ±1.45
Sacharomyces cerevaceae	19 ±0.32	13 ±2.33
Candida albicans	17 ±1.77	14 ±1.06

In vitro antifungal activity of methanolic extracts of L. speciosa and kanamycin discs

Ni-Ag NPs using plant extract of L. speciosa

Tables showing the inhibitory effects of Ni-Ag NPs against various infections and comparisons with two conventional antibiotics, Streptomycin and Ketoconazole, are available. For bacteria,the zone of inhibition (cm) of Ni-Ag nanoparticles activity varied from 0.6 to 2, while for fungus, it was 0.7 to 1.8. Below, Antibacterial activity of different concentrations of synthesized Ni-Ag NPs (25- 95µl) and control (Streptomycin 10mg/ml).

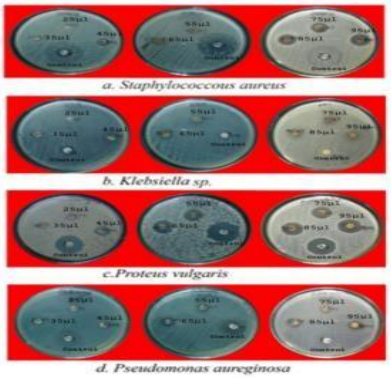

Figure 9

In addition to antibiotics, the substantial impact of Ni-Ag NPs was examined against a wide range of harmful bacteria and fungi that had developed resistance to several drugs. The exact way that silver colloid particles kill bacteria is an issue of much debate. Ni-Ag NPs have the potential to bind to cell membranes and disrupt their fundamental functions, including respiration and permeability. It is logical to assume that the accessible surface area for contact determines the bacterial particle-to-bacteria binding.

Because of their greater surface area accessible for contact, smaller particles will have a greater bactericidal impact than bigger ones. The antibacterial activity of colloidal silver particles is proportional to their size; smaller particles have a stronger bactericide impact than larger ones. Because of this, it's not out of the question that the Ag nanoparticles may infect bacteria and fungi once they get inside by interacting with sulphur- and electron-containing molecules like DNA. Toxic to bacteria, viruses, and other microbes that are resistant to several drugs are silver nanoparticles made from plants. This demonstrates their enormous promise for use in the biological field. Also, the medicinal benefits of herbal plants are amplified using silver nanoparticles, which increase their therapeutic potency.

Figure 10

Antifungal activity of different concentrations of synthesized Ni-Ag NPs (60- 100µl) and control (Ketoconozole 10mg/ml).

Table 3

Test organisms		Different Concentrations of Synthesized AgNPS (µl)							
	(Antibiotic Sterptomycin10mg/ml)	25	35	45	55	65	75	85	95
		Zone of inhibition (cm)							
Control	2.3								
Staphylococcus aureus		0.6	0.8	1.0	1.1	1.4	1.4	1.5	1.6
Control	2.5								
Proteus vulgaris		0.9	0.7	1.2	1.7	1.8	1.7	2.0	1.8
Control	-								
Klebsiella sp.		-	-	-	0.7	1.0	1.2	1.5	1.6
Control	2.0								
Pseudomonas aeruginosa		-	-	-	1.0	1.2	1.0	1.4	1.4

Antimicrobial activities of synthesized Ni-Ag NPs from L. speciosa against different bacterial Pathogens.

Table 4

Test organisms	Different Concentrations of Synthesized AgNPS (µl)					
	(Antibiotic Ketoconozole 10mg/ml)	60	70	80	90	100
		Zone of inhibition (cm)				
Control	-					
Cladosporium sp.		0.9	0.7	1.0	1.2	1.3
Control	1.4					
Aspergillus flavus		0.7	1.0	1.3	1.5	1.6
Control	1.3					
Aspergillus niger		-	-	-	-	-
Control	0.8					
Curvularia sp.		1.2	1.4	1.6	1.5	1.8

Antifungal activities of synthesized Ni-Ag NPs from L. speciosa against different fungal Pathogens.

Supporting the traditional usage of the plant in many illnesses, our investigation has shown that the methanolic extracts of L. speciosa's leaves and barks contain strong antibacterial, antioxidant, and cytotoxic potential. Researchers in this work were able to synthesise Ni-Ag NPs with the help of the medicinally significant lichen plantaginea as a possible agent for decreasing and stabilising the nanoparticles. Medical uses and industrial scale manufacturing both benefited from the biosynthesis of silver nanoparticles. The antibacterial investigations also point to the possibility of using the silver nanoparticels derived from L. speciosa as a therapeutic candidate for a range of illnesses. So synthesized Ni-Ag NPs from L. speciosa has a superior antimicrobial activity than methanolic extracts from the plants of L. speciosa.

Discussion

Antimicrobial efficacy against many pathogenic bacteria is increased by green synthesised silver nanoparticles. A new avenue in the quest for antibacterial drugs has opened thanks to the environmentally friendly method of synthesising silver nanoparticles, which has great promise in the fight against human diseases (Zaman & Hussain, 2017).

Conclusion

Overall, the environmentally friendly approach was used to synthesise the Ni-Ag nanoparticles. Through morphological analysis, they have uncovered the size, shape, and functional groupings of particles. When tested against two different types of bacteria, the biosynthesized Ls-Ni-Ag NPs showed significant antibacterial activity. In this work, researchers synthesised Ni-Ag nanoparticles utilising the Banaba plant in an environmentally friendly way and then analysed their shape using scanning electron microscopy. Results from scanning electron microscopy show that, in contrast to heat and stir synthesis, the morphology of the silver nanoparticle was transparent during heat synthesis.

Acknowledgement

We would like to thank Vels university (Pallavaram), Chennai, India for their support in all respect.

Conflict of interest

The authors declare that they have read the policy and guidelines of the journal and there is no conflict of interest.

References:

1 Sundararajan, Ranjitha kumari,2014, IJPPS,0975-1491
2. Motahher A. Qaeed. Saudi Journal of Biological Sciences 2024, 31 (1), 103899.
3. Moeng G. Motitswe, Omolola E. Fayemi, Helen P. Drummond. Journal of Cluster Science 2021, 32 (3) , 683-692..
4. Karthik C, Punnaivalavan KA, Prabha SP, Caroline DG. Int Nano Lett. 2022;12(4):313-344
5 Shereen MA, Ahmad A, Khan H, Satti SM, Kazmi A, Bashir N, Shehroz M, Hussain S, Ilyas M, Khan MI, Niyazi HA, Zouidi F., Heliyon. 2024, 15;10(6):e28038
6 Chandrakala, V., Aruna, V. & Angajala, G. Emergent Mater., 2022, 5, 1593–1615
7 Bajpay A, Nainwal RC, Singh D, Tewari SK, Med Plants, 2018, 10(3): 165-70
8 Vinit Prakash, Harpreet Kaur, Anjana Kumari, Manoj Kumar, Sumeet Gupta and

and Ritu Bala, Oriental journal of chemistry.2021,2231-5039
9 Gupta Amresh, Vipin Kumar Agarwal, Chandana Venkateswara Rao, Journal of Traditional and Complementary Medicine, 2018, 8, 164-169
10 AE Al-Snafi, International Journal of Current Pharmaceutical Research, 2019, 11 (5), 1-13
11 Muhammad Zahoor, Muhammad Nisar, Sayyed Ijazul Haq, Muhammad Ikram, Noor Ul Islam, Mohammad Naeem, Amal Open Chemistry 2023;
12 Rajya Lakshmi Koduru, P. Srinivasa Babu, I. Vikram Varma, G. Girija Kalyani and P. Nirmala, Pharmaceutical Chemistry, - 522213
13 Motahher A.Qaeed, Saudi Journal of Biological Sciences,2023.103899
14 Olivia M. Tandrasasmita ,Guntur Berliana, Raymond R. Tjandrawinata Biomedicine & Pharmacotherapy journal ,2023, 103899.
15 Mamta Devi, Shikha Devi, Vaishali Sharma, Nidhi Rana, Ravi Kant Bhatia, Arvind Kumar Bhatt, 2019, 10.1016.
16 Faisal Bin Rahman, Sium Ahmed, Priya Noor, Mir Md. Mahbubur Rahman, S.M. Azimul Huq, National library of medicine, 2020, 100805
17 Kariyellappa Nagaraja Shashiraj, Anil Hugar, Raju Suresh Kumar , Muthuraj Rudrappa Prabhakara Bhat, Abdulrahman .Almansour , Karthikeyan Perumal , PMC JOURNAL,2023 10070821.
18 Wang,Wenchuang HeXuezhu Liao, Jin Ma, Wei Gao,Haoqi ,Wang Dili Wu ,Luke R. and Cuihua Gu, Horticultural Plant Journal,2023 345-355
19. B. Prajwala, T. S. Gopenath, N. Prasad, S. Raviraja and M. K. Basalingappa IJPSR (2021),
20 Siddhant Jain and Mohan Singh Mehata, PMC JOURNAL,2019 2017
21 Priya Banerjee, Mantosh Satapathy, Aniruddha Mukhopahayay & Papita Das, Bioresources and Bioprocessing ,(2014)
22. Marvit Osman Widdatallah, Alaa Abdulmoneim Mohamed, Ayat Ahmed Alrasheid, Hiba Abbas Widatallah, Layla Fathi Yassin, Sahar Hussein Eltilib, Shimaa Abdel Rahman Ahmed,Scientific research open access journal,2020
23. vinit Prakash, harpreet kaur, anjana kumari, manoj kumar, sumeet gupta and ritu bala, oriental journal of chemistry, 2021,10.4236
24.Prajwala B and Kanthesh, Journal of Biomedical Sciences2018; 5(2): 10-17.
25. Jain S and Mehata SM: Scientific Reports 2017; 7: 1-13.
26. Dhama K and Tiwari R International Journal of Pharmacology 2014; 10: 1-43.
27. Sandhu A and Bharadwaj International Journal of Applied Biology and Pharmaceutical Technology 2013; 3(4): 310-16.
28. Prajwala B and Raghu N: Guduchi its medicinal properties. Journal of Plant Physiology & Pathology 2019;7 (3): 1-6.
29. Agarwal S and Priyadarshini, Dental Research Journal 2019; 8: 16-24.
30. Singh K and Manj Panghal, Journal of J Nanomedicine & Nanotechnology 2014; 5(2):1-6.
31. Dev SS and Vineetha KU, International Journal of Pharmaceutical Sciences and Research 2018; 9(9): 3897-02.
32. Balouiri M and Sadiki Journal of Pharmaceutical Analysis 2016; 6: 71-79.
33. Selvam K and Sudhakar, Journal of Radiation Research.2009
34. Zaman SB and Hussain 2017; 9(6): 1-9.
35. Anju, Indian Journal of Pharmacy Research and Technology2013: 3(4); 11-16.